Journal of Southeast University (English Edition) Vol. 31, No. 3, pp. 389 - 395 Sept. 2015 ISSN 1003—7985

Application of gray-tone difference matrix-based features of pavement macrotexture in skid resistance evaluation

Miao Yinghao Chen Guanghui Wang Wentao Gong Xiuqing

(Beijing Key Laboratory of Traffic Engineering, Beijing University of Technology, Beijing 100124, China)

Abstract: This paper presents a method to characterize asphalt pavement macrotexture using the gray-tone difference matrix (GTDM) and discusses the potentials of the GTDM indicators for skid resistance evaluation. There are 37 field sites included in the data collection, which cover 6 types of asphalt pavement surfaces. The mean profile depth derived from 3-D macrotexture measurements (M_{PD3}) has a significant relationship with the mean texture depth (M_{TD}), which can be described by a logarithm model with R^2 of 0.962. There is no significant linear relationship between the friction coefficient at a speed of 60 km/h (D_{FT60}) and macrotexture indicators. A nonlinear model with British pendulum number (B_{PN}) incorporated can relate D_{FT60} to M_{TD} or indicator f_{con}. A comparison with M_{TD} shows that GTDM-based f_{con} has a potential to be a macrotexture indicator for skid resistance evaluation, which describes the general height difference and the average local height difference of pavement macrotexture. A relatively high f_{con} is helpful for improving asphalt pavement skid resistance.

Key words: asphalt pavement; 3-dimensional macrotexture; gray-tone difference matrix (GTDM); skid resistance

doi: 10.3969/j.issn.1003-7985.2015.03.016

Pavement macrotexture is an important factor impacting skid resistance, which is involved in traffic safety. An appropriate evaluation of macrotexture could be helpful in understanding and increasing pavement skid resistance, thereby enhancing traffic safety[1-3]. The mean texture depth (M_{TD}) and the mean profile depth (M_{PD}) are usually employed to evaluate pavement macrotexture in practice. With the development of 3-dimensional (3-D) data acquisition techniques, researchers have been looking for approaches to collect 3-D digital macrotexture and to capture features of macrotexture based on 3-D measurements.

Cackler et al.[4] developed a 3-D macrotexture collecting system, "RoboTex", and employed the maximum texture depth derived from the 3-D measurement to evaluate cement concrete pavement macrotexture for noise mitigation. Abbas et al.[5] reconstructed the 3-D macrotextures of cement concrete pavement specimens using X-ray computerized tomography (CT) scanning. Four mathematical methods, the Hessian model, the fast Fourier transform, the wavelet analysis, and the spectral density, were used to characterize the macrotextures. Ech et al.[6] acquired the 3-D data of asphalt mixture specimens' surfaces before and after repeated loading tests using a laser-based device in laboratory. Then they evaluated the durability of macrotexture using statistical and geostatistical indicators. Gendy et al.[7] developed a system to reconstruct pavement macrotexture in 3-D based on four-source photometric stereo technique and calculated M_{PD} based on the 3-D measurement. The system was improved and named as "PhotoTexture 2.0" in 2011[8]. Vilaca et al.[9] designed a 3-D macrotexture acquisition system, "TaxScan", using laser triangulation technique. They also employed M_{PD} to characterize the macrotexture. Wen[10] acquired 3-D data of pavement macrotexture using a 3-D optical scanner, XJTUOM, in laboratory and tried to obtain M_{TD} from the measurement. Some commercial 3-D laser scanners were also applied to collect pavement macrotexture data in laboratory and field[11-12]. Moreover, some researchers developed vehicle-mounted 3-D devices to achieve a higher test speed[13-14].

It is possible to collect 3-D digital macrotexture in laboratory or in field now. Some indicators based on 3-D measurement extend the options for macrotexture evaluation. In the image processing field, texture analysis is usually used to extract the features of image. The 3-D measurement of macrotexture can be transformed into an image through mapping the heights of it onto a gray-tone set. Then the methods of texture analysis can be used for characterizing the 3-D macrotexture. Amadasun et al.[15] proposed the neighborhood gray-tone difference matrix (NGTDM), usually called GTDM, and introduced 5 indicators for analyzing texture properties. The GTDM-based indicators are effective in extracting image texture features in many fields[16-18]. They may be effective in capturing pavement macrotexture features.

This paper focuses on how to quantify the GTDM-based features of asphalt pavement macrotexture from 3-D digital measurements collected in field and the investiga-

Received 2014-12-17.

Biography: Miao Yinghao (1975—), male, doctor, associate professor, miaoyinghao@bjut.edu.cn.

Foundation item: The National Natural Science Foundation of China (No. 50908004, 51178013).

Citation: Miao Yinghao, Chen Guanghui, Wang Wentao, et al. Application of gray-tone difference matrix-based features of pavement macrotexture in skid resistance evaluation[J]. Journal of Southeast University (English Edition), 2015, 31(3): 389 - 395. [doi: 10.3969/j.issn.1003-7985.2015.03.016]

tion of the potentials of GTDM indicators of 3-D macrotexture for pavement skid resistance. First, the background of GTDM is briefly introduced. Secondly, the data collection in field is elaborated, which covers 6 types of asphalt pavements. Thirdly, the asphalt pavement macrotexture is characterized by GTDM indicators and expanded M_{PD} according to the 3-D measurements. Finally, the potentials of GTDM indicators are examined through investigating the relationship between the friction coefficient at a speed of 60 km/h (D_{FT60}) and macrotexture indicators with the British pendulum number (B_{PN}) incorporated.

1 Background of GTDM

In fact, the GTDM is a column vector, in which the i-th entry is the sum of gray-tone differences between each pixel with gray-tone i and the average gray-tone over its neighbors[15]. Denote digital gray-tone image as $I = \{G(x, y),\ x = 1, 2, \ldots, N_x,\ y = 1, 2, \ldots, N_y\}$, where $G(x, y)$ is the gray-tone at the location of (x, y), N_x and N_y are the sizes of image at directions of x and y, respectively. A gray-tone difference set as $D = \{D(x, y),\ x = D_N + 1, D_N + 2, \ldots, N_x - D_N,\ y = D_N + 1, D_N + 2, \ldots, N_y - D_N\}$ can be calculated by

$$D(x,y) = \left| G(x,y) - \frac{1}{(2D_N+1)^2-1} \cdot \left[\left(\sum_{i=x-D_N}^{x+D_N} \sum_{j=y-D_N}^{y+D_N} G(i,j) \right) - G(x,y) \right] \right| \quad (1)$$

where $D(x,y)$ is the difference of the $G(x,y)$ with the average gray-tone over its neighbors; D_N is the neighborhood size in pixel. We divide D into a series of subsets as $D_i = \{D(x,y):\ G(x,y) = i\}$, $i = 1, 2, \cdots, N_g$, where N_g is the maximum gray-tone of I. The sum of D_i is the i-th entry of the GTDM, $S(i)$. If D_i is empty, assign 0 to $S(i)$. Fig. 1 depicts an example of the calculation of GTDM with $D_N = 1$.

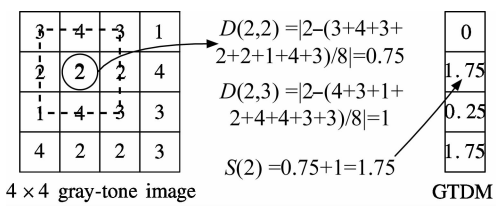

Fig. 1 An example of GTDM calculation

Amadasun et al.[15] proposed five feature indicators based on the GTDM, which are coarseness, contrast, busyness, complexity, and strength[19]. For convenience, I is divided into 2 subsets as I_E and I_C, which consist of all pixels on the 4 edges with width of D_N and the other pixels, respectively. The coarseness is defined as[19]

$$f_{cos} = \left[\varepsilon + \sum_{i=1}^{N_g} p_i S(i) \right]^{-1} \quad (2)$$

where ε is a small number to prevent f_{cos} becoming infinite; p_i is the occurrence probability of gray-tone i in I_C, which can be calculated by

$$p_i = \frac{N_{D_i}}{n_p} \quad (3)$$

where N_{D_i} is the element number of D_i; n_p is the pixel number of I_C, which can be calculated by

$$n_p = (N_x - 2D_N)(N_y - 2D_N) \quad (4)$$

The contrast is defined as[19]

$$f_{con} = \left[\frac{1}{n_g(n_g-1)} \sum_{i=1}^{N_g} \sum_{j=1}^{N_g} p_i p_j (i-j)^2 \right] \left[\frac{1}{n_p} \sum_{i=1}^{N_g} S(i) \right] \quad (5)$$

where

$$n_g = \sum_{i=1}^{N_g} Q_i, \qquad Q_i = \begin{cases} 1 & p_i \neq 0 \\ 0 & p_i = 0 \end{cases} \quad (6)$$

The busyness, complexity, and strength are defined as follows[19]:

$$f_{bus} = \frac{\sum_{i=1}^{N_g} p_i S(i)}{\sum_{i=1}^{N_g} \sum_{j=1}^{N_g} |ip_i - jp_j|} \qquad p_i \neq 0,\ p_j \neq 0 \quad (7)$$

$$f_{com} = \sum_{i=1}^{N_g} \sum_{j=1}^{N_g} \frac{|i-j|}{n_p(p_i+p_j)} [p_i S(i) + p_j S(j)] \qquad p_i \neq 0,\ p_j \neq 0 \quad (8)$$

$$f_{str} = \frac{\sum_{i=1}^{N_g} \sum_{j=1}^{N_g} (p_i + p_j)(i-j)^2}{\varepsilon + \sum_{i=1}^{N_g} S(i)} \qquad p_i \neq 0,\ p_j \neq 0 \quad (9)$$

2 Data Collection

Field tests are conducted at 37 sites, which are selected from highways of various grades and urban roads in Huairou and Chaoyang Districts, Beijing, China. They cover 6 types of asphalt pavement surfaces, dense asphalt concrete (DAC), stone matrix asphalt (SMA), rubber asphalt concrete (RAC), ultra-thin wearing course (UTWC), micro-surfacing (MS), and open graded friction course (OGFC). The basic information of the test sites is listed in Tab. 1. The pavement surface is scanned using a commercial hand held 3-D laser scanner. The macrotexture is presented by a point set with a sample size of 90 mm × 90 mm and a sample interval of 0.5 mm in two horizontal directions. The test method is explained in Ref. [20]. Fig. 2 gives a typical 3-D macrotexture. M_{TD}, B_{PN}, and D_{FT60} were also collected using the sand patch method (ASTM E 965), the British pendulum tester

(ASTM E 303), and dynamic friction tester (DFT) (ASTM E 1911), respectively. B_{PN} were not collected for all OGFC and 2 RAC test sites; D_{FT60} were not collected for all OGFC test sites. All the tests were conducted in situ in November 2010 except OGFC test sites, which were tested in May 2012. A new set of rubber pads for DFT was replaced and used for all tests in November 2010. Before the tests in May 2012 were conducted, the rubber pads of the DFT underwent several other tests. It also should be noted that maybe the asphalt film was not totally worn off for the test sites opening in 2010 when the tests were conducted even though most aggregates had emerged.

Tab. 1 Basic information of the test sites

Highway coding	Grade	Surface type	NMPS/mm	Number of test sites	Opening date
G101	1	SMA	13.2	5	Aug. 2010
	1	UTWC1	9.5	4	Sept. 2009
	1	UTWC2	9.5	4	Sept. 2010
	1	MS	9.5	4	Sept. 2009
G111	2	DAC1	16.0	7	July 2010
	2	RAC	16.0	6	Sept. 2010
X011	3	DAC2	13.2	3	Sept. 2009
JCXL	Urban road	OGFC	13.2	4	June 2008

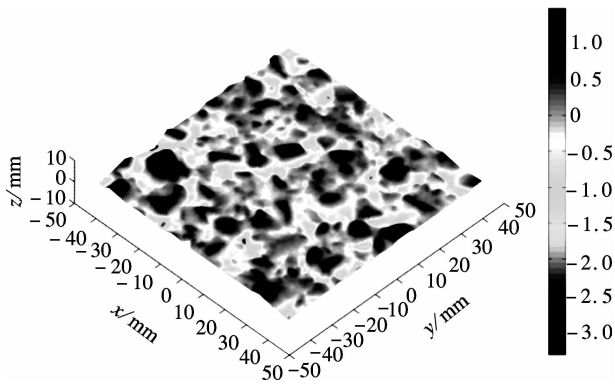

Fig. 2 A typical 3-D macrotexture

3 Characterizing Asphalt Pavement Macrotexture

3.1 GTDM indicators

The 3-D measurement of macrotexture can be converted into a gray-tone image by dividing the height range into sections with a given interval and mapping each section onto a gray-tone. Then, it can be characterized by the GTDM indicators. This paper employs an interval of 0.05 mm, which is the accuracy of the depth of the 3-D scanner. The conversion is described as

$$G(x,y) = \text{floor}\left(\frac{Z(x,y) - \min(Z)}{0.05}\right) + 1 \qquad (10)$$

where (x,y) is the location of the point or pixel in the macrotexture; $Z(x,y)$ is the height at the location of (x, y), mm; floor(·) rounds a number to the nearest integer less than or equal to it. Fig. 3 depicts the gray-tone image corresponding to the macrotexture shown in Fig. 2. The GTDM indicators are calculated with $D_N = 1$ for each macrotexture.

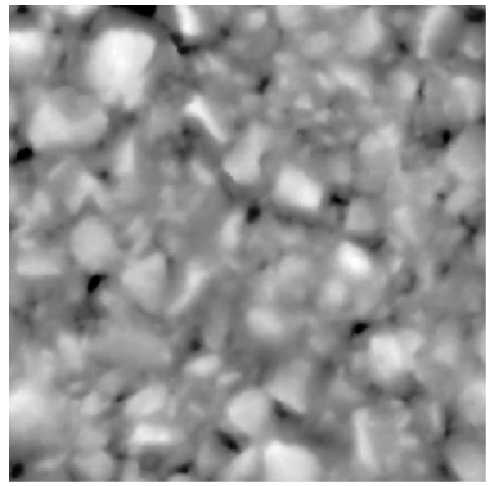

Fig. 3 The gray-tone image corresponding to the macrotexture shown in Fig. 2

3.2 Mean profile depth

M_{PD} is widely used to evaluate the pavement macrotexture in practice and some researchers attempted to calculate M_{PD} according to 3-D measurement[7,12]. The 3-D measurement of the macrotexture usually can be divided into a series of parallel profiles. Considering each profile in the 3-D measurement as a segment, we can obtain an indicator like M_{PD} through averaging the mean depths of all profile segments. It is called M_{PD3} hereinafter to discriminate it from the profile-based M_{PD}. In this paper, the 3-D measurement of macrotexture can be divided into 181 segments along x or y axis. The values of M_{PD3} are calculated based on the segments divided along x and y axis, respectively. The mean of the 2 values is adopted as the final value of M_{PD3} to eliminate the orientation effect. Fig. 4 depicts a typical profile segment and its mean depth, which is extracted from a 3-D measurement[21].

Fig. 5 depicts the relationship between M_{PD3} and M_{TD},

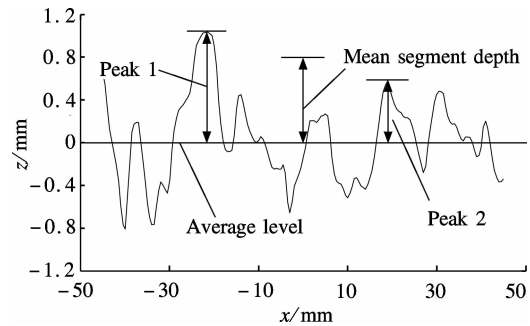

Fig. 4 A typical profile and its mean segment depth

which can be captured by the following logarithm model:

$$M_{TD} = 0.526\ 3\ln(M_{PD3} - 0.938\ 3) + 1.386\ 1 \quad (11)$$

The analysis of variance for the logarithm model is presented in Tab. 2. It is shown that the model is highly significant. The mean square error (MSE) of the model is 0.002 27 and R^2 is 0.962.

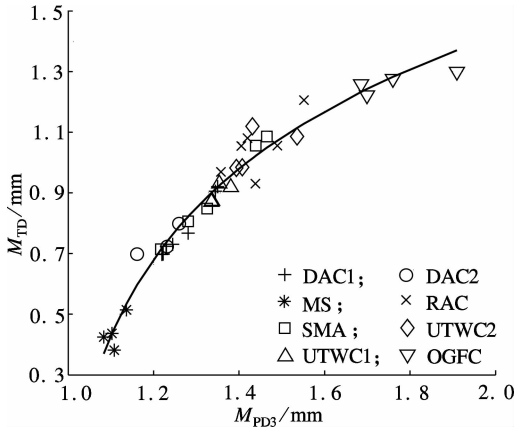

Fig. 5 Scatter plot of M_{TD} against M_{PD3} with the logarithm regression model

Tab. 2 Analysis of variance for the logarithm model relating M_{TD} and M_{PD3}

Source	Degree of freedom	Sum of squares	Mean square	F value	Significance level
Model	2	1.939 6	0.969 8	426.51	<0.000 1
Error	34	0.077 3	0.002 27		
Corrected total	36	2.016 9			

4 Relationship between GTDM Indicators and Skid Resistance

This paper investigates the relationships between GTDM indicators, M_{PD3}, M_{TD}, B_{PN} and D_{FT60}, using correlation analysis. Tab. 3 lists the Pearson correlation coefficient matrix. Among the 5 GTDM indicators, f_{con} has the maximum correlation coefficient of 0.727 5 with D_{FT60}, while the others just have values below 0.3. The correlation coefficients between D_{FT60} and M_{TD}, M_{PD3} are 0.448 3 and 0.406 3, respectively, which are much less than that between f_{con} and D_{FT60}. Fig. 6 gives the scatter plots of D_{FT60} with f_{con}, M_{TD} and M_{PD3}. According to Tab. 3 and Fig. 6, there is no significant linear relationship between D_{FT60} and the macrotexture indicators. The Penn state model[22] is usually used to describe the nonlinear relationship between the friction coefficients and slip speed with consideration of the macrotexture influence. To investigate the potential of f_{con} in macrotexture evaluation for skid resistance, this paper incorporates B_{PN} to relate D_{FT60} and macrotexture indicators with referring to the Penn state model.

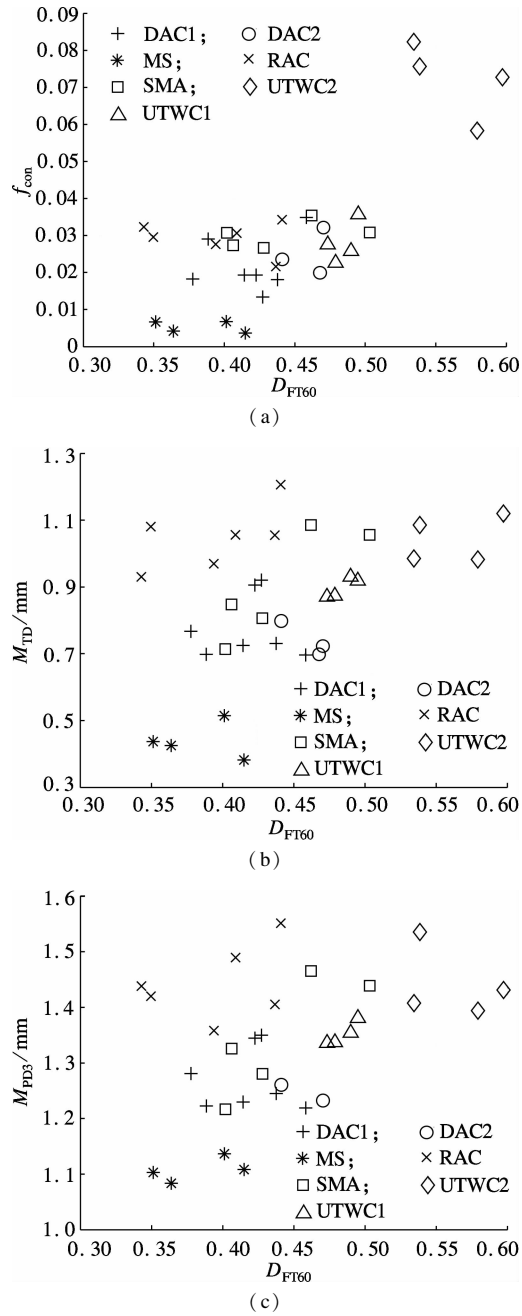

Fig. 6 Scatter plots of D_{FT60} against f_{con}, M_{TD} and M_{PD3}. (a) D_{FT60}-f_{con}; (b) D_{FT60}-M_{TD}; (c) D_{FT60}-M_{PD3}

The models of relationships between D_{FT60} and M_{TD}, f_{con} with B_{PN} incorporated are described by Eqs. (12) and (13), respectively. Tabs. 4 and 5 present the results of analysis of variance for the two models. It is shown that both the two models are significant. The MSEs of the models with M_{TD} and f_{con} are 0.002 6 and 0.002 4, respectively. Figs. 7 and 8 depict the measured D_{FT60} with the predicted D_{FT60} by Eqs. (12) and (13), respectively. According to the comparison with M_{TD}, the GTDM-based f_{con} shows a potential to be a macrotexture indicator for skid resistance evaluation.

$$D_{FT60} = B_{PN}\exp\left(\frac{-1}{0.006\ 2M_{TD} + 0.200\ 4}\right) \quad (12)$$

Tab. 3 Pearson correlation coefficient matrix

Indicators	D_{FT60}	B_{PN}	M_{TD}	M_{PD3}	f_{cos}	f_{con}	f_{bus}	f_{com}	f_{str}
D_{FT60}	1.000 0	0.608 6	0.448 3	0.406 3	−0.147 7	0.727 5	−0.285 2	0.139 1	−0.193 1
B_{PN}	0.608 6	1.000 0	0.399 0	0.336 2	−0.094 6	0.565 3	−0.407 1	0.151 0	−0.129 8
M_{TD}	0.448 3	0.399 0	1.000 0	0.933 9	0.057 8	0.742 8	−0.494 9	0.832 1	0.351 7
M_{PD3}	0.406 3	0.336 2	0.933 9	1.000 0	−0.164 5	0.765 4	−0.317 3	0.790 8	0.182 8
f_{cos}	−0.147 7	−0.094 6	0.057 8	−0.164 5	1.000 0	−0.365 6	−0.485 7	0.131 6	0.787 1
f_{con}	0.727 5	0.565 3	0.742 8	0.765 4	−0.365 6	1.000 0	−0.236 2	0.578 1	−0.13 70
f_{bus}	−0.285 2	−0.407 1	−0.494 9	−0.317 3	−0.485 7	−0.236 2	1.000 0	−0.457 9	−0.519 5
f_{com}	0.139 1	0.151 0	0.832 1	0.790 8	0.131 6	0.578 1	−0.457 9	1.000 0	0.608 1
f_{str}	−0.193 1	−0.129 8	0.351 7	0.182 8	0.787 1	−0.137 0	−0.519 5	0.608 1	1.000 0

Tab. 4 Analysis of variance for the exponential model with M_{TD}

Source	Degree of freedom	Sum of squares	Mean square	F value	Significance level
Model	2	6.162 4	3.081 2	1 183.7	<0.000 1
Error	29	0.075 5	0.002 6		
Uncorrected total	31	6.237 9			

Tab. 5 Analysis of variance for the exponential model with f_{con}

Source	Degree of freedom	Sum of squares	Mean square	F value	Significance level
Model	2	6.169 7	3.084 9	1 312.6	<0.000 1
Error	29	0.068 2	0.002 4		
Uncorrected total	31	6.237 9			

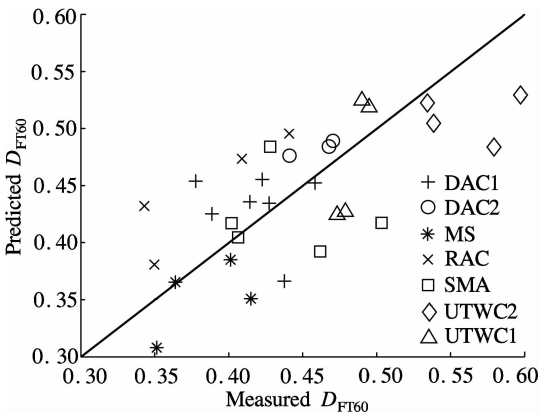

Fig. 7 Measured D_{FT60} against predicted D_{FT60} by M_{TD}

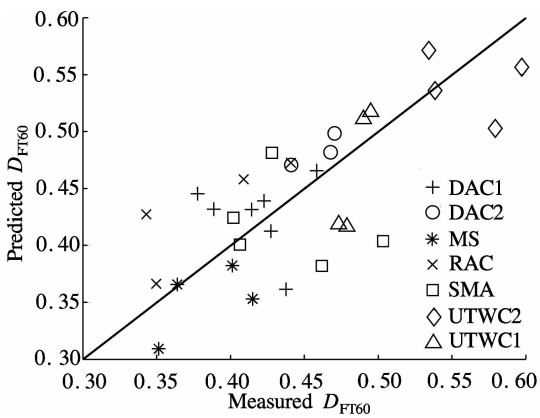

Fig. 8 Measured D_{FT60} against predicted D_{FT60} by f_{con}

$$D_{FT60} = B_{PN}\exp\left(\frac{-1}{0.094\ 3f_{con} + 0.202\ 7}\right) \tag{13}$$

5 Discussion

It is helpful to investigate the meaning of f_{con} for pavement macrotexture. Denote

$$f_1 = \frac{1}{n_g(n_g-1)}\sum_{i=1}^{N_g}\sum_{j=1}^{N_g} p_i p_j (i-j)^2 \tag{14}$$

$$f_2 = \frac{1}{n_p}\sum_{i=1}^{N_g} S(i) \tag{15}$$

Then

$$f_{con} = f_1 f_2 \tag{16}$$

Define a pixel pairs set corresponding to I_C as $P = \{[G(r,s),G(t,u)]: r,\ t = D_N+1, D_N+2,\cdots,N_x - D_N;\ s,\ u = D_N+1, D_N+2,\cdots,N_y - D_N\}$. P can be divided into a series of subsets as $P_{ij} = \{[G(r,s),G(t,u)]: G(r,s)=i,\ G(t,u)=j\}$, $i = 1,2,\cdots,N_g$; $j = 1,2,\cdots,N_g$. Then $p_i p_j$ is the element number proportion of P_{ij} to P. Therefore, the summation part of Eq. (14) is the average of gray-tone difference square over all pixel pairs in P. According to Eq. (6), we know that n_g is the number of gray-tones actually existing in I_C. The summation part in Eq. (14) is normalized through dividing it by $n_g(n_g-1)$. Thus, we know that f_1 is the normalized average of gray-tone difference square over all pixel pairs in P. It represents the general height difference of the pavement macrotexture.

According to the definition of GTDM, $S(i)$ is the sum of D_i. Then

$$\sum_{i=1}^{N_g} S(i) = \sum_{x=1+D_N}^{N_x-D_N}\sum_{y=1+D_N}^{N_y-D_N} D(x,y) \tag{17}$$

Therefore,

$$f_2 = \frac{\sum_{x=1+D_N}^{N_x-D_N}\sum_{y=1+D_N}^{N_y-D_N} D(x,y)}{(N_x-2D_N)(N_y-2D_N)} \tag{18}$$

Actually, Eq. (18) is the average of D. We can clearly understand that f_2 is the average of gray-tone differ-

ences between all pixels and the mean over their neighbors. It represents the average local height difference of the pavement macrotexture. According to the previous analysis, it is known that the indicator f_{con}, the product of f_1 and f_2, captures both the general and local height differences of pavement macrotexture.

6 Conclusion

According to the 3-D measurement of asphalt pavement macrotexture, this paper quantifies its features using the GTDM indicators. Expended M_{PD} (M_{PD3}) is also calculated using the 3-D measurements. The potentials of the GTDM indicators for skid resistance evaluation are investigated by comparing them with the traditional macrotexture indicators according to data collected in situ, which covers 6 types of asphalt pavement surface, DAC, SMA, RAC, UTWC, MS, and OGFC. Results show that the M_{PD3} has a strong relationship with M_{TD}, which can be described by a logarithm model with R^2 of 0.962. Correlation analysis and the scatter plots show that there is no significant linear relationship between D_{FT60} and macrotexture indicators. A nonlinear model, referring to the Penn state model, is used to relate D_{FT60} to macrotexture indicator with B_{PN} incorporated. It is shown that the model is significant when M_{TD} or f_{con} is included as macrotexture indicator. A comparison with M_{TD} shows that the indicator f_{con} has the potential to be a macrotexture indicator for skid resistance evaluation.

The indicator f_{con} includes two components which describe the general height difference and the average local height difference of pavement macrotexture, respectively. A relatively high f_{con} is helpful for improving asphalt pavement skid resistance.

References

[1] OECD. *Towards zero: ambitious road safety targets and the safe system approach* [M]. Paris: Organization for Economic Co-operation and Development, 2008: 121.

[2] Henry J J. Evaluation of pavement friction of characteristics [R]. Washington, DC: Transportation Research Board, 2000.

[3] AASHTO. *Guide for pavement friction* [M]. Washington, DC: American Association of State Highway and Transportation Officials, 2008.

[4] Cackler E T, Ferragut T, Harrington D S. Evaluation of U. S. and European concrete pavement noise reduction methods [R]. Ames, IA, USA: National Concrete Pavement Technology Center, Iowa State University, 2006.

[5] Abbas A, Kutay M E, Azari H, et al. Three-dimensional surface texture characterization of portland cement concrete pavements [J]. *Computer-Aided Civil and Infrastructure Engineering*, 2007, **22**(3): 197 - 209.

[6] Ech M, Yotte S, Morel S, et al. Laboratory evaluation of pavement macrotexture durability [J]. *Revue Européenne de Génie Civil*, 2007, **11**(5): 643 - 662.

[7] Gendy A E, Shalaby A. Mean profile depth of pavement surface macrotexture using photometric stereo techniques [J]. *Journal of Transportation Engineering*, 2007, **133**(7): 433 - 440.

[8] Gendy A E, Shalaby A, Saleh M, et al. Stereo-vision applications to reconstruct the 3D texture of pavement surface [J]. *International Journal of Pavement Engineering*, 2011, **12**(3): 263 - 273.

[9] Vilaca J L, Fonseca J C, Pinho A M, et al. A new machine for acquire pavement texture [C]//*IEEE 7th International Conference on Computational Cybernetics*. Palma de Mallorca, Spain, 2009: 97 - 102.

[10] Wen J. Study on evaluating texture depth of asphalt pavement with digital technology [D]. Xi'an: School of Information Engineering, Chang'an University, 2009.

[11] Bitelli G, Simone A, Girardi F, et al. Laser scanning on road pavements: a new approach for characterizing surface texture [J]. *Sensors*, 2012, **12**: 9110 - 9128.

[12] Sengoz B, Topal A, Tanyel S. Comparison of pavement surface texture determination by sand patch test and 3D laser scanning [J]. *Periodica Polytechnica: Civil Engineering*, 2012, **56**(1): 73 - 78.

[13] Wang K C P, Li L. Pavement surface texture modeling using 1 mm 3d laser images [C]//*Transportation Systems Workshop*. Austin, TX, USA, 2012.

[14] Laurent J, Hébert J F, Lefebvre D, et al. Using 3d laser profiling sensors for the automated measurement of road surface conditions [C]//*7th RILEM International Conference on Cracking in Pavements*. Delft, Netherlands, 2012.

[15] Amadasun M, King R. Textural features corresponding to textural properties [J]. *IEEE Transactions on Systems, Man and Cybernetics*, 1989, **19**(5): 1264 - 1274.

[16] Vince D G, Dixon K J, Cothren R M, et al. Comparison of texture analysis methods for the characterization of coronary plaques in intravascular ultrasound images [J]. *Computerized Medical Imaging and Graphics*, 2000, **24**(4): 221 - 229.

[17] Christodoulou C I, Michaelides S C, Pattichis C S. Multifeature texture analysis for the classification of clouds in satellite imagery [J]. *IEEE Transactions on Geoscience and Remote Sensing*, 2003, **41**(11): 2662 - 2668.

[18] Nurzyńska K, Kubo M, Muramoto K. Texture operator for snow particle classification into snowflake and graupel [J]. *Atmospheric Research*, 2012, **118**: 121 - 132.

[19] Materka A, Strzelecki M. Texture analysis methods—a review [R]. Brussels: Institute of Electronics, Technical University of Lodz, 1998.

[20] Miao Y H, Song P P, Gong X Q. Fractal and multifractal characteristics of 3D asphalt pavement macrotexture [J]. *Journal of Materials in Civil Engineering*, 2014, **26**(8): 04014033.

[21] ASTM. E1845-09 Standard practice for calculating pavement macrotexture mean profile depth [S]. West Conshohocken: ASTM International, 2009.

[22] Wambold J C, Antle C E, Henry J J, et al. International PIARC experiment to compare and harmonize texture and skid resistance measurements [R]. Paris: Permanent International Association of Road Congresses, 1995.

路面宏观纹理灰度差异矩阵特征在抗滑评价中的应用

苗英豪　陈广辉　王文涛　宫秀青

（北京工业大学北京市交通工程重点实验室，北京 100124）

摘要：为了改善对路面宏观纹理特征的评价，用灰度差异矩阵（GTDM）刻画了沥青路面宏观纹理，并探讨了基于 GTDM 的特征指标在抗滑性能评价中应用的可行性. 数据采集包含 37 个路面现场测点，涵盖 6 种类型的沥青路面. 基于三维宏观纹理数据的平均断面深度（M_{PD3}）与平均纹理深度（M_{TD}）有显著的相关关系，指数关系模型的 R^2 为 0.962. 路面宏观纹理指标与 60 km/h 速度下的摩擦系数（D_{FT60}）之间没有显著的线性关系. 一个包含摆式摩擦系数测试仪测试结果（B_{PN}）的非线性模型可以将 D_{FT60} 与 M_{TD} 或指标 f_{con} 联系起来. 与 M_{TD} 相比较，基于 GTDM 的 f_{con} 作为宏观纹理指标在抗滑性能评价中具有可用性，f_{con} 描述了路面纹理总的高差情况和平均局部高差情况. 较高的 f_{con} 值有益于提高沥青路面抗滑性能.

关键词：沥青路面；三维宏观纹理；灰度差异矩阵；抗滑性能

中图分类号：U416.2